Discriminant Analysis of Autofluorescence Spectra for Classification of Oral Lesions In Vivo

J.L. Jayanthi, MSc, MPhil,[1] Rupananda J. Mallia, MSc,[1] Sara Thomas Shiny, MSc,[1] Kamalsanan V. Baiju, MSc,[2] Anitha Mathews, MD,[3] Rejnish Kumar, MD,[3] Paul Sebastian, MS,[3] Jayaprakash Madhavan, MD,[3] G.N. Aparna, MSc, MPhil,[1] and Narayanan Subhash, MSc, PhD[1]*

[1]*Biophotonics Laboratory, Centre for Earth Science Studies, Akkulam, Trivandrum 695 031, Kerala, India*
[2]*Department of Statistics, Sree Narayana College, Chempazhanthy, Trivandrum 695 587, Kerala, India*
[3]*Regional Cancer Centre, Medical College, Trivandrum 695 011, Kerala, India*

Background and Objectives: Low survival rate of individuals with oral cancer emphasize the significance of early detection and treatment. Optical spectroscopic techniques are under various stages of development for diagnosis of epithelial neoplasm. This study evaluates the potential of a multivariate statistical algorithm to classify oral mucosa from autofluorescence spectral features recorded in vivo.

Study Design/Methods: Autofluorescence spectra were recorded in a clinical trial from 15 healthy volunteers and 34 patients with diode laser excitation (404 nm) and preprocessed by normalization, mean-scaling and its combination. Linear discriminant analysis (LDA) based on leave-one-out (LOO) method of cross validation was performed on spectral data for tissue characterization. The sensitivity and specificity were determined for different lesion pairs from the scatter plot of discriminant function scores.

Results: Autofluorescence spectra of healthy volunteers consists of a broad emission at 500 nm that is characteristic of endogenous fluorophores, whereas in malignant lesions three additional peaks are observed at 635, 685, and 705 nm due to the accumulation of porphyrins in oral lesions. It was observed that classification design based on discriminant function scores obtained by LDA-LOO method was able to differentiate pre-malignant dysplasia from squamous cell carcinoma (SCC), benign hyperplasia from dysplasia and hyperplasia from normal with overall sensitivities of 86%, 78%, and 92%, and specificities of 90%, 100%, and 100%, respectively.

Conclusions: The application of LDA-LOO method on the autofluorescence spectra recorded during a clinical trial in patients was found suitable to discriminate oral mucosal alterations during tissue transformation towards malignancy with improved diagnostic accuracies. Lasers Surg. Med. 41:345–352, 2009. © 2009 Wiley-Liss, Inc.

Key words: laser-induced autofluorescence spectroscopy; clinical trials; discriminant function scores; classification of oral tissues

INTRODUCTION

Oral cavity cancer is a major health concern the world over. India has one of the highest incidences of oral cancer in the world and it ranks first in males and third in females [1,2]. This is primarily associated with the habit of betel quid chewing, pan, and tobacco usage of a large population in India. In spite of advancements in the field of cancer detection and therapy, the 5-year survival rate of oral cancer patients is still below 60%. Oral pre-malignant lesions often present as white patches (leukoplakia) or as red patches (erythroplakia) with a risk for conversion to malignancy of approximately 10% and 90%, respectively. Progression from pre-malignant to cancerous condition takes place usually over many years, which can be prevented if detected in its formative stages. The delay in diagnosis may be partly due to the ignorance of public about the symptoms of oral pre-cancer and the need for routine oral cancer screening.

Proper management of patients with pre-malignant or malignant oral lesion often starts with its accurate diagnosis. The widely accepted diagnostic method is visual examination followed by biopsy and histopathological evaluation of the suspicious lesion. To ensure accurate diagnosis the biopsy site must be selected carefully. But, even for experienced clinicians, it is difficult to find the optimum site for biopsy since suspicious oral lesion often varies in disease severity from one part of the lesion to another. For example, a lesion may have early invasive squamous cell carcinoma (SCC) in one part and mild dysplasia in another. An appropriate biopsy would include tissue from the worst part of the lesion. Therefore, accurate histopathological diagnosis depends on the clinician doing an appropriate biopsy and providing adequate clinical information, and on the pathologist correctly interpreting the biopsy results [3]. Because of the complexity of the head and neck region multiple or repeated biopsies are not possible. Since biopsy is painful and pathological analysis time consuming there is a need to develop

alternate methodologies for in vivo detection and real-time diagnosis of oral pre-malignancies.

Development of a non-invasive method for real-time screening of neoplastic changes and diagnosis of oral cavity lesions have great potential to improve the quality of life and survival rate of oral cancer patients. Autofluorescence spectroscopy is an innovative diagnostic modality that reduces the need of repeated biopsies and unlike biopsy; the screening can be carried out repeatedly in vivo. The technique involves illumination of suspicious lesions with monochromatic light and recording the fluorescence spectra emitted by endogenous tissue fluorophores such as nicotinamide adenine dinucleotide (NADH), collagen, elastin, keratin, flavin adenine dinucleotide (FAD), and porphyrins. The presence of disease results in alteration in concentration of these fluorophores as well as the light scattering and absorption properties of tissue, nuclear size distribution, collagen content, and epithelial thickness, which leads to the spectral variations [4].

Fluorescence spectroscopy has been used successfully as in vivo and in vitro techniques for fast and non-invasive detection of cancers and pre-cancers in a variety of organ systems including cervix, bronchus, breast, esophagus, colon, skin, and oral cavity [5–12]. De Veld et al. [13] have given an extensive review of literature and presented the status of autofluorescence spectroscopy and imaging in the diagnosis of oral lesions in vivo. The spectral information is compared with histopathological reports, and algorithms were developed to classify tissues based on histology, thereby enabling fast, non-invasive, automated screening, and diagnosis in a clinical setting [14].

Multivariate analytical methods were used for spectral analysis by various research groups in cancer detection [15–17]. Ramanujam et al. [15] combined principal component analysis (PCA) and logistic regression for classification of human cervical tissue fluorescence acquired in vivo and reported an overall sensitivity of 88% and specificity of 70% to differentiate squamous intraepithelial lesions (SILs) from normal squamous epithelia and inflammation. Using partial least squares (PLS) and artificial neural network (ANN) based classification model, Wang et al. [16] obtained a sensitivity of 81% for recognizing pre-malignant and malignant tissues and a specificity of 96% for identifying benign samples that consists of normal, oral submucous fibrosis and epithelial hyperplasia. Kamath and Mahato [17] have discussed the potential of fluorescence spectroscopy for detection of oral carcinomas in vitro by classification of the spectra by PCA and k-means nearest neighbor analysis and obtained a specificity, sensitivity, and accuracy of 100%, 94.5%, and 96.2%, respectively. Manjunath et al. [18] reported that PCA using Mahalanobis distance and spectral residuals provide best discrimination among oral tissues using autofluorescence. All these studies reveal the capability of multivariate analytical methods in classification of tissues from autofluorescence spectral data.

Discriminant analysis (DA) has been performed by many groups for spectral data analysis [19–21]. Following ex vivo studies, Wang et al. used partial least squares discriminant analysis (PLSDA) with cross validation to analyze in vivo spectral data from hamster buccal pouch lesions. Their studies showed that by choosing proper thresholds, PLSDA with cross validation provides an identification rate of 86% for hyperkeratosis, 87% for normal, and 89% for dysplastic samples [19].

In this study we explore the potential of linear discriminant analysis (LDA) to predict group membership of a sample with unknown group. The discriminant function scores determined by LDA based on leave-one-out (LOO) method were used to find a cut-off value for discriminating normal from hyperplasia, hyperplasia from dysplasia and dysplasia from SCC lesions. Towards this, we have recorded in vivo laser-induced autofluorescence (LIAF) spectra of oral lesions from patients and healthy volunteers using a point monitoring fiber-optic device and utilized LDA-LOO method for real-time discrimination oral mucosa and the results are presented.

MATERIALS AND METHODS

Study Population

Autofluorescence spectra were recorded from 15 healthy volunteers with no clinically observable lesions and 34 patients having different grades of malignancy. An experienced physician specialized in radiation oncology identified lesions for spectral studies and records its visual imprint. Measurements were carried out at the out patient clinic of the Regional Cancer Centre (RCC), Trivandrum after getting approval of the Ethical Committee of RCC. Patients were asked to sign an informed consent prior to measurements. All the patients included in this study had prolonged habits of either pan chewing, smoking, or alcohol consumption, while healthy population maintained good oral hygiene with none of the above habits.

Experimental Setup

The LIAF system used for in vivo measurements is shown in Figure 1. This system consists of a 404 nm, 50 mW diode laser (Stocker Yale, Montreal, Canada) for excitation of fluorescence and a fiber-optic spectrometer (Ocean Optics, Inc., Dunedin, FL; Model: USB 2000FL VIS-NIR) connected to the USB port of a laptop for recording of tissue fluorescence. Light emission from the laser source is guided to the lesion through a 3-m long bifurcated fiber-optic probe (Ocean Optics, Inc.; Model: ZR400—5-VIS/NIR) that has a central fiber to deliver the excitation light to the lesion and six surrounding fibers (400 μm diameter each) to collect the fluorescence emission. In order to maintain the fluorescence intensity incident on the spectrometer CCD within safe limits the laser power at the probe tip was maintained at 1 mW. The fiber-optic probe was terminated in a stainless steel ferrule of 15 cm length and 6 mm diameter for easy access to the oral cavity and to enable sterilization with boiling water, before and after use. A flexible 10 mm long, disposable, black PVC sleeve was inserted at the probe tip to avoid ambient light from entering the detection system and to provide extra hygiene. The separation between the probe tip and the sample was optimized (by sliding the PVC
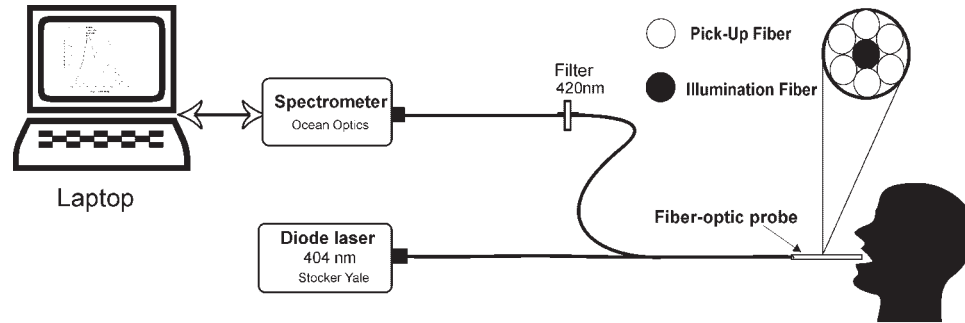
Fig. 1. Schematic of the experimental set up for LIAF measurements.

sleeve over the ferrule) to a distance of 3.5 mm; wherein the excitation beam completely overlaps the collection area. A long pass filter (Schott GG420) was used during fluorescence measurements to block the back-scattered laser light from entering the spectrometer. The spectrum was recorded in the 420−720 nm wavelength region using the OOI Base32 software supplied by Ocean Optics, Inc., configured to record the spectra, averaged for 40 scans, with a boxcar width of 10 nm and an integration time 100 milliseconds. The experimental system is explained in detail elsewhere [22].

Study Protocol

Before measurements, all patients and healthy volunteers were asked to rinse their mouth with 0.9% saline solution for 2 minutes in order to reduce the effect of recently consumed food. They were also provided with protective goggles to shield their eyes against laser light. After 15 sets of spectral measurements from a typical site covering an area of 6 mm diameter, a punch biopsy (2×2 mm^2 approximately in size) was taken from the central portion of the measurement site. The biopsy slides were prepared and classified by an experienced pathologist who was blinded to the autofluorescence spectral results. In the case of healthy volunteers, visual impression was carried out instead of biopsy. After measurements, the spectroscopic results were correlated with histopathological findings.

Data Processing

Autofluorescence spectral data recorded from different oral cavity sites of patients/volunteers were categorized based on pathological reports as normal (15 healthy volunteers), hyperplasia (10 patients), dysplasia (9 patients), and SCC (15 patients). Randomly selected 29 samples belonging to these categories with known group membership (pathological results) were used as a training/prediction set and the remaining 20 samples with unknown group membership were used for validation. Data pre-processing methods such as normalization, mean-scaling, and normalization cum mean-scaling were used to find out whether there is any spectral enhancement due to pre-processing [15]. Spectra from each patient was averaged and then normal-

ized individually to the maximum fluorescence intensity of each spectrum. Mean-scaling was performed by calculating the mean of each sample and then subtracting this mean from each spectrum, and the resultant value represents the difference in fluorescence at a particular site with respect to the average spectrum.

Statistical Analysis

Principal component analysis. PCA is a multivariate statistical technique that is used for compressing a larger data set without losing the strength of data. Since the fluorescence intensity data set extends from 420−720 nm (with three values for each nm), we used PCA to identify the orthogonal components of the spectra with maximum variance within the complete data set. LDA was then performed on the extracted significant principal components to determine the discriminant function scores. Each principal component is co-related to the spectral variables of the original fluorescence emission and provides insight into the spectral features that contribute to the classification [6,15]. An independent sample Student's t-test was carried out for testing the significance of mean PC scores between different tissue categories.

Linear discriminant analysis. Discriminant function is a latent variable which is created as a linear combination of discriminating variables, such that $L = b_1 x_1 + b_2 x_2 + \cdots + b_n x_n + c$, where b's are the discriminant coefficients, the x's are the discriminating variables, and c is a constant. The linear discriminant function transforms the original PC scores on the sample into a single discriminant score, which represents the sample position along a line defined by the linear discriminant function. Functions are generated from a sample of cases for which group membership is known, and these are then applied to new cases with unknown group membership. This classification based on LOO method of cross validation produces a confusion matrix that compares predicted versus actual group membership.

The extracted significant principal components with P-value <0.005 are used as the input variables for DA, which produces a classification table to assess how well the discriminant function works. In order to assess the significance of the discriminant function scores the Wilks Lambda test was used. Since the discriminant scores are

predictors of group membership for classifying observations, we have performed a blind-test using the remaining 20 samples to assess the suitability of the training data set.

RESULTS

Spectral Features

In vivo autofluorescence spectral measurements were carried out on consenting healthy volunteers and patients. Figure 2 shows the fluorescence spectra averaged for different tissue categories and normalized with respect to the maximum spectral intensity around 500 nm. Marked differences in spectral features are observed between healthy and diseased tissues. The broad autofluorescence peak at 500 nm arising from endogenous fluorophores is characteristic of all epithelial tissues. The 635 nm peak is more prominent in lesions diagnosed as SCC as compared to dysplastic and hyperplastic tissues. In addition two peaks are also seen at 685 and 705 nm that are absent in healthy tissues. Another notable feature is the broadening of the 500 nm peak towards red wavelength region in dysplastic tissues.

Correlation between each principal component and variables of the normalized fluorescence emission spectrum are studied with the help of the component-loading plot. Figure 3 shows loadings of the first three PCs for all the lesions studied. PC1 represents the mean autofluorescence spectrum for all lesions. PC2 and PC3 look similar to the porphyrin like peaks around 635 and 705 nm and also
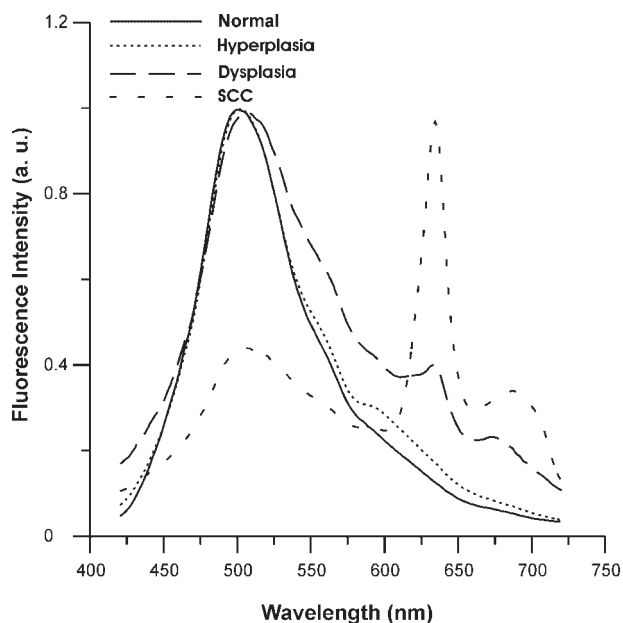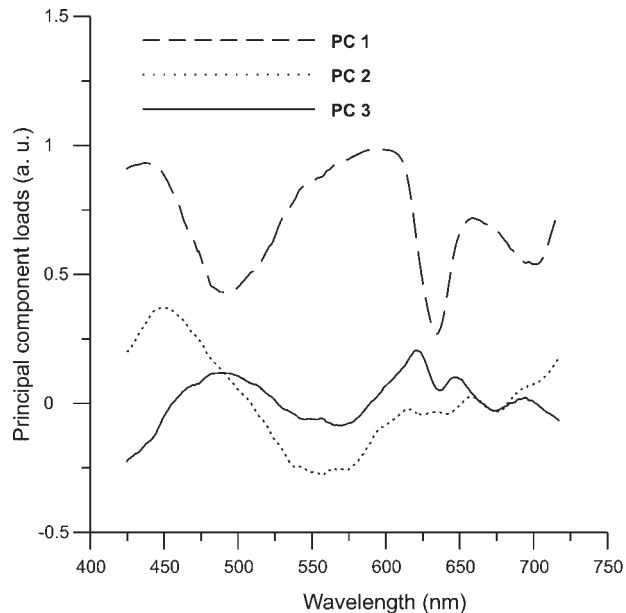
Fig. 3. First three principal components of different lesion groups included in the analysis. Each averaged spectrum was normalized with respect to the emission peak intensity.

show dips at 545 and 575 nm due to oxygenated hemoglobin absorption in blood. These three PCs jointly give a variance of 98.6% to the spectra.

Linear Discriminant Analysis

Pair-wise DA was performed on the extracted significant principal components from the training set. Scatter plots were drawn based on the discriminant function scores obtained (Fig. 4a–c). Since the scores obtained by LDA can either be negative or positive, the scatter plot for each pair is given separately. The cut-off value in the scatter plot, which is the weighted mean of the paired values, is used to classify different lesions. The cut-off values for normal–hyperplastic, hyperplastic–dysplastic, SCC–dysplastic pairs are 0.241, 0.188, and −0.191, respectively. Diagnostic accuracies such as sensitivity, specificity, positive and negative predictive values for each pair were calculated by correlating the position of discriminant function scores for each lesion in the scatter plot with the corresponding histopathological result. The sensitivities obtained for normal–hyperplasia, hyperplasia–dysplasia, and dysplasia–SCC pairs are 83%, 80%, and 89% respectively and the corresponding specificities are 100%, 100%, and 80%, respectively (Table 1).

In order to test the reliability of the classification procedure used, a blind-test was carried out in 20 patients with unknown group membership. Discriminant function scores of the blind test data were inserted into the scatter plot of the training set for validation and the results are correlated with histopathological findings. It was observed that the developed algorithm could correctly classify ten samples of normal–hyperplastic pairs, seven samples out

Fig. 2. LIAF emission from the oral mucosa of 34 patients and 15 healthy volunteers. Normal spectra show the average of 15 measurements carried out at 11 anatomical sites in 15 healthy volunteers, whereas hyperplasia, dysplasia, and SCC spectra are the mean of 15 measurements each in 10, 9, and 15 patients, respectively.
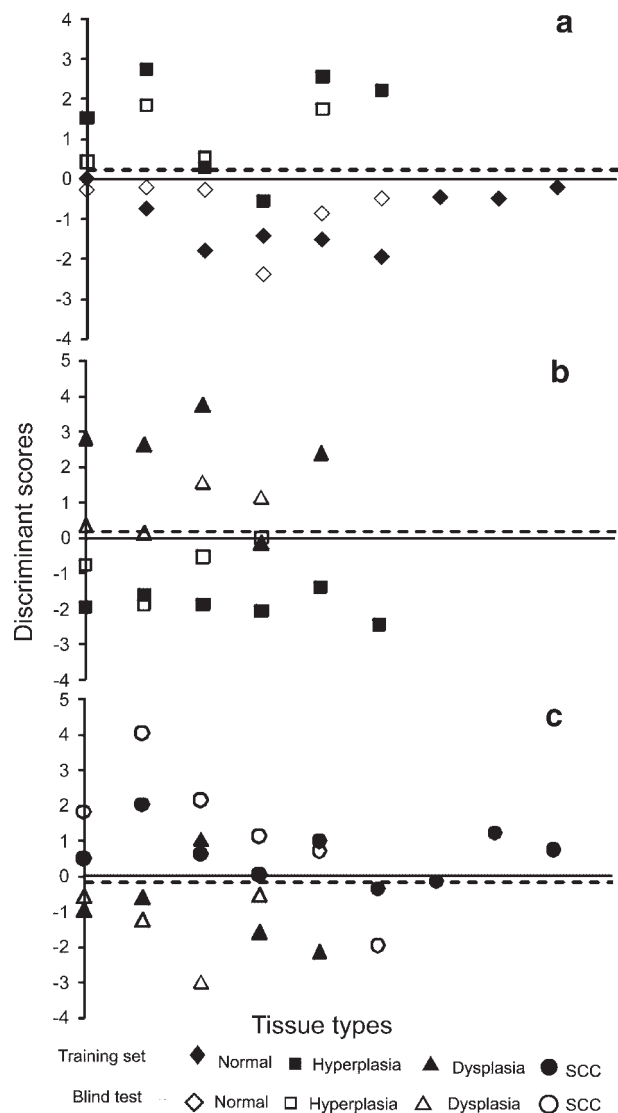
Fig. 4. Pair-wise scatter plot based on discriminant function scores for 15 healthy volunteers and 34 patients with different lesion types. (**a**) Normal–hyperplasia, (**b**) hyperplasia–dysplasia, and (**c**) dysplasia–SCC. The solid symbols represent the results of training data set and the open symbols relate to the validation data set. The dotted line represents the cut-off value for each lesion pair.

of eight dysplastic-hyperplastic pairs (with one dysplastic case misclassified as hyperplasia) and nine samples out of ten dysplastic-SCC pairs (with one case of SCC misclassified as dysplasia). This leads to a specificity of 100% and sensitivity of 100%, 75%, and 83% respectively for normal–hyperplasia, hyperplasia–dysplasia, and dysplasia–SCC lesion pairs in the blind-test (Fig. 4a–c).

The overall sensitivity, specificity, accuracy, positive predictive value (PPV) and negative predictive value (NPV) calculated from the scatter plots (Fig. 4a–c) are given in Table 1. We were able to discriminate pre-malignant

dysplastic lesions from malignant SCC with 86% sensitivity, and 90% specificity, whereas for discriminating hyperplasia from normal and hyperplasia from dysplasia, the sensitivities were 92% and 78% respectively, with 100% specificity.

DISCUSSION

The autofluorescence peak at 500 nm has been reported as due to emission from endogenous fluorophores like NADH, FAD, collagen, elastin, and amino acids, while the emissions at 635 and 705 nm are from enhanced occurrence PpIX in malignant tissues [22–24]. The additional peak seen at 685 nm in SCC and dysplastic lesions (Fig. 2) is due to the accumulation of coproporphyrin III, a constituent of the heme synthesis pathway in malignant tissues [22].

Earlier studies have shown that measurement from healthy tissues within a patient is not well defined, due to "field cancerization" through the influence of carcinogens like tobacco, pan, and alcohol [16,22,25]. Therefore, the present study relied on spectral measurements from healthy population as control and attained improved sensitivities and specificities for tissue discrimination (Table 1). Nevertheless, sites such as vermilion border (VB) of the lip, dorsal, and lateral sides of the tongue could not be studied due to the presence of porphyrin/bacteria emissions at 635, 685, and 705 nm [22,25].

While different methods were used for pre-processing of spectral data, normalization with respect to the autofluorescence peak intensity was found to give better results in classification. In comparison, mean-scaling of spectral data and mean-scaling of normalized data did not improve the classification efficiency.

First three PC loadings (Fig. 3) of the spectral data set resembled the average autofluorescence spectrum (PC1), oxygenated hemoglobin absorption dips and porphyrin like peaks (PC2 and PC3) observed with excitation at 404 nm. The three PCs together form 98.6% of the variance in the spectra, which means that the complete spectral data set could well be described by these three PCs. The significant difference observed in the mean PC scores (P-value <0.005) between different lesions, with minimum standard deviation, shows that tissue classification is possible with the information contained in these PCs. The shape of the PC loading is responsible for the observed significant differences.

In this clinical trial, we have obtained an overall sensitivity of 92%, 78%, and 86% respectively for discriminating normal from benign, benign from pre-malignant and pre-malignant from malignant tissues with corresponding specificities of 100%, 100%, and 90% (Table 1). Since grade of malignancy could vary from one point in a lesion to another and the biopsy samples were taken from a smaller portion of the measured site, the sensitivities and specificities reported are lower (Table 1).

In comparison, using PLS–ANN classification algorithm, Wang et al. [16] obtained a sensitivity of 81% and a specificity of 96% for discrimination of pre-malignant and

TABLE 1. Overall Diagnostic Accuracies Obtained for Different Lesion Pairs Consisting of 29 Samples in the Training (Prediction) Set and 20 Samples in the Validation (Blind Test) Data Set

Lesion pairs	Normal vs. hyperplasia					Hyperplasia vs. dysplasia					Dysplasia vs. SCC				
	Se (%)	Sp (%)	Acc (%)	PPV (%)	NPV (%)	Se (%)	Sp (%)	Acc (%)	PPV (%)	NPV (%)	Se (%)	Sp (%)	Acc (%)	PPV (%)	NPV (%)
Training set	83	100	93	100	90	80	100	91	100	86	89	80	86	89	80
Validation set	100	100	100	100	100	75	100	88	100	80	83	100	90	100	80
Overall	92	100	97	100	95	78	100	90	100	83	86	90	88	95	80

Sensitivity (Se) = true positive/(true positive + false negative), specificity (Sp) = true negative/(true negative + false positive), accuracy (Acc) = (true positive + true negative)/(positive + negative), positive predictive value (PPV) = true positive/(true positive + false positive), negative predictive value (NPV) = true negative/(true negative + false negative).

malignant from benign tissues. Similarly, a sensitivity of 92% and a specificity of 95% was obtained for discriminating benign from dysplasia or SCC using PLSDA of autofluorescence spectral data for in vivo diagnosis of hamster buccal pouch pre-cancers and cancers [19]. In comparison, De Veld et al. [26] reported a sensitivity of 94% and a specificity of 94% for distinguishing cancerous lesions from normal.

For group classification, LDA is a well-established method, which unites input parameters into a discriminant function to classify the available data into different groups [20,21]. In this study PCA was performed only for the reduction of spectral intensity data. Tissue classification was made purely based on the discriminant function scores obtained by LDA for each lesion. Cut-off values in the scatter plot were used to calculate diagnostic accuracies. The results obtained show the ability of this procedure to act as an adjuvant to clinicians for in vivo tissue differentiation in real-time without any tissue removal.

The discriminant function scatter plot is shown in Figure 5 for all the four groups. In this figure the first two functions in LDA classifies the lesions into four different groups based on group centroids. Group means are centroids and differences in location of centroids represent dimensions along which the groups differ. It is possible to visualize discrimination between groups by plotting the individual scores for the two discriminant functions. This classification based on the Mahalanobis distance is a multivariate measure of the separation of a point from the mean of a dataset in n-dimensional space. The sample is classified to the group from which it has shorter Mahalanobis distance. All the normal and SCC lesions are classified correctly in Figure 5 while there is an overlap in the case of hyperplasia and dysplasia samples. One dysplasia sample was misclassified as SCC, whereas one hyperplasia was misclassified as normal and another one as dysplasia. Rectangular boxes are drawn to demarcate each group. The error bars of the mean discriminant function scores at 95% confidence interval are plotted in Figure 6. It can be seen that there is no overlap between different groups and this shows the statistical significance between different groups and also confirms the classification potential of the mean discriminant function scores. The

results presented reveal the potential of this method to accurately discriminate different lesion types using discriminant function scores.

CONCLUSION

The present study using LDA on the autofluorescence spectral data obtained in a clinical setting from oral mucosa was able to classify dysplasia from SCC, dysplasia from
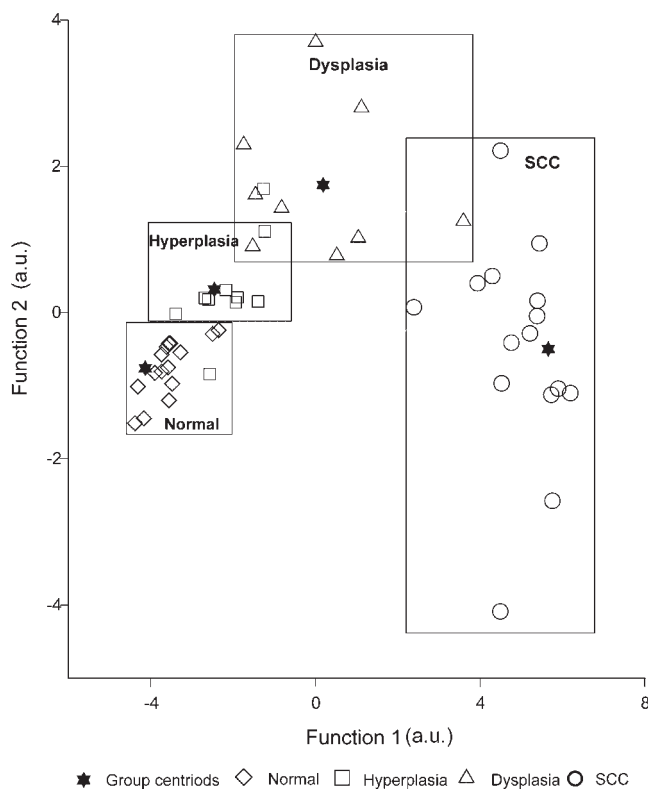
Fig. 5. Scatter plot of the first two discriminant functions by LDA. The four categories of oral tissues are located in the four distinct areas. The results are presented according to the discriminant function scores determined based on LOO method of cross validation.
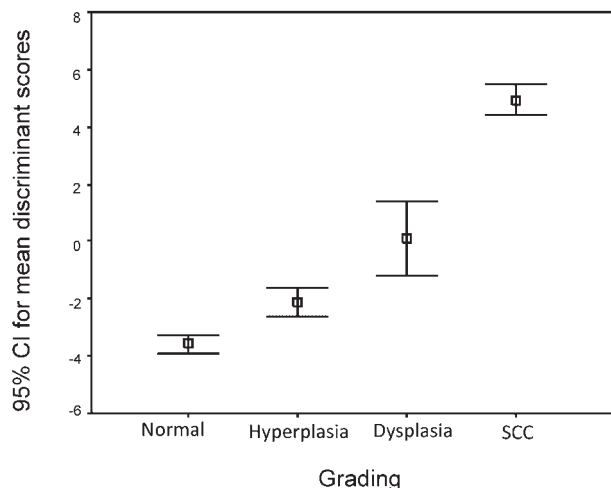
Fig. 6. Discriminant function scores plotted with their error bars for different lesions at 95% confidence interval for the mean.

hyperplasia and hyperplasia from normal with sensitivities of 92%, 78%, and 86%, respectively with corresponding specificities of 100%, 100%, and 90%. The results obtained show improved sensitivity and specificity as compared to previous reports and confirm the advantages of using multivariate statistical analysis on LIAF spectral data for non-invasive diagnosis of oral pre-malignancies. Further measurements are envisaged in a larger population to explore the applicability of discriminant functions for grading of oral mucosa in real-time and to improve the diagnostic accuracies for discrimination of hyperplastic and dysplastic lesions from normal and to distinguish oral submucous fibrosis from other pre-malignant conditions.

ACKNOWLEDGMENTS

REFERENCES

1. Hamada GS, Bos AJ, Kasuga H, Hirayama T. Comparative epidemiology of oral cancer in Brazil & India. Tokai J Exp Clin Med 1991;16(1):63–72.
2. Sankaranarayanan R. Oral caner in India: An epidemiologic and clinical review. Oral Surg Oral Med Oral Path 1990;69: 325–330.
3. Poh CF, Ng S, Berean KW, Williams PM, Rosin MP, Zhang L, Biopsy and histopathologic diagnosis of oral pre-malignant and malignant lesions. JCDA Clin Pract 2008;74(3):283–288.
4. Wu Y, Qu JY. Autofluorescence spectroscopy of epithelial tissues. J Biomed Opt 2006;11(5):054023(1–11).
5. Majumder SK, Ghosh N, Kataria S, Gupta PK. Nonlinear pattern recognition for laser-induced fluorescence diagnosis of cancer. Lasers Surg Med 2003;33:48–56.
6. Ramanujam N, Mitchell MF, Mahadevan A, Thomsen S, Malpica A, Wright T, Atkinson N, Richards-Kortum R. Spectroscopic diagnosis of cervical intraepithelial neoplasia (CIN) in vivo using laser-induced fluorescence spectra at multiple excitation wavelengths. Lasers Surg Med 1996;19: 63–74.
7. Panjehpour M, Overholt BF, Vo-Dinh T, Haggitt RC, Edwards DH, Buckley FP. Endoscopic fluorescence detection of high-grade dysplasia in barrett's esophagus. Gastroentrology 1996;111:93–101.
8. Zellweger M, Grosjean P, Goujon D, Monnier P, Van den Bergh H, Wagnieres G. Invivo autofluorescence spectroscopy of human bronchial tissue to opimize the detection and imaging of early cancers. J Biomed Opt 2001;6(1):41–51.
9. Breslin TM, Xu F, Palmer GM, Zhu C, Gilchrist KW, Ramanujam N. Autofluorescence and diffuse reflectance properties of malignant and benign breast tissues. Ann Surg Oncol 2004;11(1):65–70.
10. Schomacker KT, Frisoli JK, Compton CC, Flotte TJ, Richter JM, Nishioka NS, Deutsch TF. Ultraviolet laser-induced fluorescence of colonic issue: Basic biology and diagnosis potential. Lasers Surg Med 1992;12:63–78.
11. Heintzelman DL, Utzinger U, Fuchs H, Zuluaga A, Gossage K, Gillenwater AM, Jacob R, Kemp B, Richards_Kortum RR. Optimal excitation wavelengths for *in vivo* detection of oral neoplasia using fluorescence spectroscopy. Photochem photobiol 2000;72(1):103–113.
12. Ingrams DR, Dhingra JK, Roy K, Perrault DF, Bottrill ID, Kabani S, Rebeiz EE, Pankratov MM, Shapshay SM, Manoharan R, Itzkan I, Feld MS. Autofluorescence characteristics of oral mucosa. Head Neck 1997;19:27–32.
13. De Veld DCG, Witjes MJH, Sterenborg HJCM, Roodenburg JLN. The status of in vivo autofluorescence spectroscopy and imaging for oral oncology. Oral Oncol 2005;41:117–131.
14. Ramanujam N. Fluorescence spectroscopy of neoplastic and non-neoplastic tissues. Neoplasia 2000;2:89–117.
15. Ramanujam N, Mitchell MF, Mahadevan A, Thomsen S, Malpica A, Wright T, Atkinson N, Richards-Kortum R. Development of a multivariate statistical algorithm to analyze human cervical tissue fluorescence spectra acquired in vivo. Lasers Surg Med 1996;19:46–62.
16. Wang CY, Tasi T, Chen HM, Chen CT, Chiang CP. PLS-ANN based classification model for oral submucous fibrosis and oral carcinogenesis. Lasers Surg Med 2003;32:318–326.
17. Kamath SD, Mahato KK. Optical pathology using oral tissue fluorescence spectra: Classification by principal component analysis and k-means nearest neighbor analysis. J Bio Med Opt 2007;12(1):014028(1–9).
18. Manjunath BK, Kurein J, Rao L, Murali Krishna C, Chidananda MS, Venkatakrishna K, Kartha VB. Autofluorescence of oral tissue for optical pathology in oral malignancy. J Photochem Photobiol B Biol 2004;73:49–58.
19. Wang CY, Tasi T, Chen HC, Chang SC, Chen CT, Chiang CP. Autofluorescence spectroscopy for in vivo diagnosis of DMBA-induced hamster buccal pouch pre-cancers and cancers. J Oral Pathol Med 2003;32:18–24.
20. Dzendrowskyj T, Bourne R, Himmelreich U, Mountford C, Sorrell TC. Classification of cerebral infection and tumor by linear discriminant analysis of biopsy spectra. Proc Intl Soc Magn Reson Med 2001;9:2280.
21. Fernandez GCJ. Discriminant analysis, a powerful classification technique in data mining. Proc SAS conference (SUGI 27), Florida, 2002; paper 247.
22. Mallia RJ, Thomas SS, Mathews A, Kumar R, Sebastian P, Madhavan J, Subhash N. Laser-induced autofluorescence spectral ratio reference standard for early discrimination of oral cancer. Cancer 2008;112:1503–1512.

23. Richards-Kortum R, Muraca ES. Quantitative optical spectroscopy for tissue diagnosis. Annu Rev Phys Chem 1996;47: 555–606.

24. Inaguma M, Hashimoto K. Porphyrin-like fluorescence in oral cancer. Cancer 1999;86:2201–2211.

25. De Veld DCG, Skurichina M, Witjes MJH, Duin RPW, Sterenborg HJCM, Star WM, Roodenberg JLN. Autofluorescence characteristics of healthy oral mucosa at different anatomical sites. Lasers Surg Med 2003;32(5):367–376.

26. De Veld DCG, Skurichina M, Witjes MJH, Duin RPW, Sterenborg HJCM, Roodenburg JLN. Autofluorescence and diffuse reflectance spectroscopy for oral oncology. Lasers Surg Med 2005;36(5):356–364.